Sn-Bearing Minerals and Associated Sphalerite from Lead-Zinc Deposits, Kosovo: An Electron Microprobe and LA-ICP-MS Study

Joanna Kołodziejczyk [1],*, Jaroslav Pršek [1], Panagiotis Voudouris [2], Vasilios Melfos [3] and Burim Asllani [4]

[1] Department of Economic Geology, Faculty of Geology, Geophysics and Environmental Protection, AGH University of Science and Technology, al. Mickiewicza 30, Kraków 30-059, Poland; prsek@geol.agh.edu.pl

[2] Department of Mineralogy and Petrology, Faculty of Geology & Geoenvironment, National and Kapodistrian University of Athens, Athens 15784, Greece; voudouris@geol.uoa.gr

[3] Department of Mineralogy, Petrology and Economic Geology, Faculty of Geology, Aristotle University of Thessaloniki, Thessaloniki 54124, Greece; melfosv@geo.auth.gr

[4] E & E Experts LLC, Prishtina 10000, Republic of Kosovo; burimasllani@hotmail.com

* Correspondence: asia.office@wp.pl; Tel.: +48-603-166-271

Abstract: Stannite group minerals (ferrokësterite and stannite) occur in small amounts in association with sulfides in hydrothermal Pb-Zn deposits in Kosovo. The chemical composition of sphalerite co-existing with Sn-bearing minerals has been investigated using laser ablation inductively-coupled plasma mass spectrometry (LA-ICP-MS). Flat Sn-spectra suggest that Sn is bound in the sphalerite lattice or as nanoincluions. Sphalerite from Stan Terg, overgrown by ferrokësterite, contains the lowest Sn content (few ppm) and have been precipitated before Sn-enrichment in the fluids. The highest value of Sn (520 ppm) of Stan Terg sphalerite was obtained directly close to the ferrokësterite rim, and indicates a rapid increase of Sn in the hydrothermal fluids. Significantly higher values of Sn in sphalerite were obtained from other deposits: 1600 ppm (Artana), up to 663 ppm (Kizhnica), up to 2800 ppm (Drazhnje). Stannite-sphalerite geothermometry revealed the following ore-forming temperatures for the Kosovo mineralization: 240–390 °C for Stan Terg, 240–370 °C for Artana, >340 °C for Kizhnica, and 245–295 °C for Drazhnje. Sphalerite and stannite group minerals precipitated simultaneously during cooling from reduced hydrothermal fluids and under low-sulfidation fluid states. Fluctuations in physico-chemical fluid conditions are evidenced by the presence of stannite group minerals along growth zones in sphalerite and may be related to short interval of magmatic pulses during ore deposition.

Keywords: stannite group minerals; sphalerite; LA-ICP-MS study; Trepça Mineral Belt; Kosovo

1. Introduction

Tin is an economically important element with the highest concentration in Sn and W porphyry, skarn, greisen, or polymetallic vein-type deposits [1]. The most widespread Sn mineral is cassiterite, but Sn can frequently occur as sulfides (stannite, kësterite, mawsonite, *etc.*), or sulfosalts (cylindrite, franckeite, *etc.*). Tin mineralization was reported from porphyry-related and epithermal systems in China [2], Sn-Te-Bi-Sb polymetallic veins in Japan [3], polymetallic vein in Kutná Hora (Czech republic) [4], granite-related Sn-mineralization at Mount Wellington (Cornwall, Great Britain) [5], VMS-type deposit of Neves Corvo (Portugal) [6], CSA Cu-Pb-Zn deposit in Australia [7], and many others elsewhere. Catchpole *et al.* [8] assigned stannite and kësterite as accessory minerals in the

transitional Zn-Cu and distal Pb-Zn-Ag rich zones in Morococha district, Peru. Kase [9] described Sn mineral association from a Sn-As-Zn-Ag vein in the Besshi deposit, Japan, and Petruk [10] found thiostannates (stannite, kësterite, stannoidite, mawsonite) in Brunswick Tin Mines, Canada. The Lavrion Pb-Zn-Ag carbonate-replacement deposit in Southern Greece, as well as several polymetallic epithermal high-intermediate sulfidation vein-type Au-Ag deposits in Northeastern Greece, contain Sn-bearing phases (e.g., stannite, petrukite, kestërite, mohite, kuramite, colusite, *etc.*) in association with tellurides and bi-sulfosalts-sulfotellurides [11–13]. Zarić *et al.* [14] described greisen-type mineralization with cassiterite, and hydrothermal overprints with stannite, kësterite, and ferrokësterite, and high Sn content in sphalerite (up to 0.3 wt %) in the Srebrenica ore field within the Vardar Zone.

Coexisting stannite and sphalerite have been considered by numerous authors as a good geothermometer, mainly based on the chemical compositions of synthetic phases [15–17]. Shimizu and Shikazono [18] applied this method to samples from Japanese ore deposits and obtained a good correlation between stannite-sphalerite temperatures and homogenization temperatures of fluid inclusions and sulfur isotope temperatures. They pointed out that the equation given by Nakamura and Shima [17] better fits to the real temperature values. For Japanese skarn and vein deposits Shimizu and Shikazono [18] obtained temperatures between 250 and 350 °C, in agreement with data from fluid inclusions. Wagner *et al.* [19] applied this method for the San Rafael deposit (Peru) and obtained temperatures in the range 270–290 °C (slightly lower than the range from fluid inclusions). Watanabe *et al.* [20] considered that ore deposition at the Otage kaolinite-pyrophyllite deposit (Japan), took place at temperatures from 300 to 340 °C, almost equal to those from fluid inclusions in nearby quartz. Brill [7] obtained an average temperature of 264 °C for the CSA Cu-Pb-Zn deposit, Australia (lower than the temperature estimated from fluid inclusions), probably due to late metamorphic changes. Kase [9] obtained a range from 260 to 345 °C for Sn-As-Zn-Ag veins of the Besshi deposit in Japan, and Ohta [21] suggested temperatures above 300 °C for the Toyoha Pb-Zn-Ag vein deposit in Japan. Both authors decided that the Nakamura and Shima [17] equation is more relevant than the equation given by Nekrasov *et al.* [15].

The Pb-Zn hydrothermal deposits in the Trepça Mineral Belt (TMB) are an important source of base metals in Southern Europe, and tin-bearing minerals are minor but important constituents of the mineralization [22]. Generally, the Sn content in the ore concentrates from the Stan Terg mine is low, and it reaches up to 200 ppm in Zn-concentrate, and up to 120 ppm in Pb-concentrate [23]. The studied deposits belong to the same metallogenic province and are assigned to hydrothermal-metasomatic deposits. Stan Terg deposit is described as a skarn deposit by Strmić Palinkaš *et al.* [24] and by Kołodziejczyk *et al.* [25] as an example of Pb-Zn-Ag skarn, or carbonate replacement deposit type. The other Pb-Zn deposits in TMB, such as Kizhnica, Artana, and Drazhnje have not been studied in detail, however ore composition, textural and structural features of the ore are similar to those in Stan Terg indicating a similar hydrothermal origin.

This study examines intergrowths of stannite group minerals-sphalerite from Kosovo Pb-Zn deposits, and presents results on chemical composition of sphalerite coexisting with SGM obtained by electron microprobe and LA-ICP-MS analyses. The aim of the study is to establish physico-chemical conditions of ore deposition and to compare individual deposits in terms of trace element content in sphalerite and stannite group minerals that may be used for exploration activities for base and critical metals elsewhere.

2. Geological Background

The Pb-Zn deposits in Kosovo belong to the TMB and are located within the Serbo-Macedonian metallogenic province, which is part of the Vardar Zone (Figure 1). TMB stretches between Kopaonik massif in the north and ends in Kizhnica area in the south and hosts numerous Pb-Zn deposits and occurrences. The ore mineralization in this area is of Oligocene-Miocene age, and is related to the post-collisional magmatic activity in the area, being part of a NNW-trending magmatic belt

extending from Serbia through Kosovo and Former Yugoslav Republic of Macedonia to Greece [23,26]. Three regional NNW-trending zones of mineralization were recognized in the TMB [27].
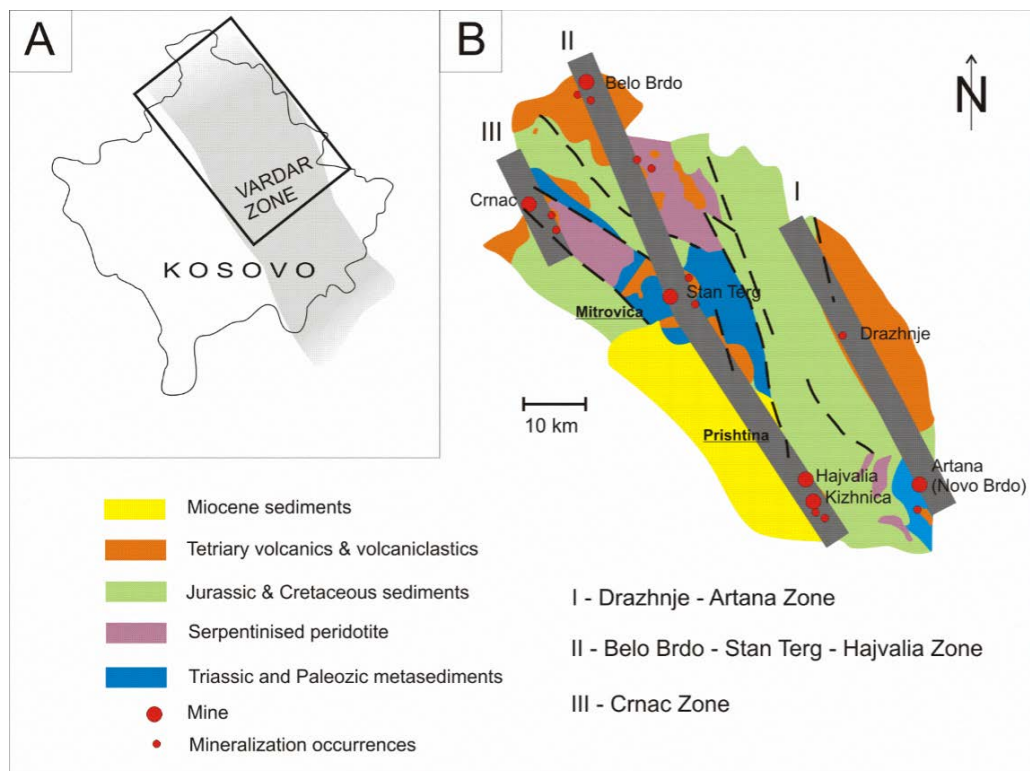
Figure 1. (**A**) Position of the Trepça Mineral Belt, (B) is marked in rectangle. (**B**) Simplified geological map of the Trepça Mineral Belt with marked mines, occurrences of Pb-Zn mineralization and three mineralized zones (thick grey lines), modified from Hyseni *et al.* [27].

2.1. Stan Terg Deposit

Stan Terg is the largest and the best recognized Pb-Zn deposit in the area, exploited since medieval times, and located 8 km northeast from Kosovska Mitrovica, in the central zone of the TMB (Figure 1). Presently, the Trepça Mining Company is carrying out an underground extraction of lead and zinc ore. The ore mineralization is of hydrothermal origin, and Stan Terg was classified as an example of Pb-Zn-Ag skarn, or a carbonate replacement deposit type [24,25,27–31]. The area is located at the southern fringe of the Kopaonic granodioritic massif and is composed of Paleozoic and Triassic metamorphic rocks and an ophiolite complex. The mineralization at Stan Terg is mostly hosted within the Upper Triassic limestones, present in the core of an anticline, and covered by schists. The ore bodies were formed parallel to the hinge of the anticline, within carbonates or at the contact between carbonates with schists and an andesitic phreatomagmatic volcanic pipe, and have a lenticularly-elongated, columnar-like shape. Skarn minerals (hedenbergite, ilvaite) are present in some of the ore bodies close to the volcanic pipe. Principal ore minerals in the Stan Terg deposit are galena, sphalerite, pyrite, pyrrhotite, arsenopyrite, boulangerite, and chalcopyrite.

2.2. Artana Deposit

Artana (Novo Brdo) deposit is located about 20 km southeast from Pristina, in the external zone of the TMB (Figure 1). The mineralization has been excavated since ancient times. The present underground mine was opened in the 20th century and operates today by Trepça Mining Company. Mineralization in the Artana deposit occurs in several ore bodies and is hosted in Paleozoic and Cretaceous sediments (mainly in crystalline limestones) at the contact with gneisses, amphibolites, and

Tertiary volcanic rocks. The mineralization has a metasomatic character and is dominated by galena, sphalerite, and pyrite. Some skarn mineralization was mentioned by Simić [32] and was supposed to occur at the contact with andesite.

2.3. Kizhnica Deposit

Kizhnica, in association with two other Pb-Zn deposits, Badovc and Ajvalia, is located about 7 km southeast of Prishtina, in the central zone of the TMB (Figure 1). The Kizhnica deposit was excavated during the 20th century as an open pit. The area is dominated by Neogene volcanic rocks (andesites), Paleozoic and Mesozoic magmatic, metamorphic, sedimentary rocks (flysh series), (Veles Series), and Pliocene sediments. The mineralization occurs at the contact zone (1600 m × 300 m wide) between a serpentinite complex and a Lower Cretaceous flysch, but is mostly located close to the volcanic rocks. The ore bodies have irregular shapes, similar to veins, lenses, or they occur as impregnations. The hydrothermal mineralization comprises sulfides (with three generations of galena and sphalerite), sulfosalts, carbonates, and quartz [33,34].

2.4. Drazhnje Deposit

The Drazhnje (Cuka e Batlavë) deposit is located in the Eastern Kosovo, 23 km northeast from Prishtina, in the external zone of the TMB (Figure 1). The area belongs to the western margin of the Lece massif and is composed of andesite-dacite volcanics and pyroclastics of the Late Mesozoic-Early Tertiary age [35]. The Lece intrusive complex has intruded a folded Cretaceous sedimentary sequence, as well as metamorphosed Paleozoic-Mesozoic rocks (mainly schists and carbonates) and small serpentine lenses of Jurassic age [32,35]. The mineralization has mostly a hydrothermal-metasomatic character and occurs in the form of stockworks, impregnations, and also filling fractures in carbonates [32]. Main ore minerals are sphalerite, boulangerite, galena, pyrite, and marcasite. About 4 million tonnes of Pb-Zn ore with Pb + Zn content above 6% has been documented. The analyzed samples came from the Saint George ore body.

3. Methods

Sphalerite-stannite intergrowths in representative ore samples were determined by a JEOL JXA-8230 Super Probe electron microprobe (EPMA) (JEOL, Tokyo, Japan) in the Critical Elements Laboratory at the Faculty of Geology, Geophysics, and Environmental Protection, AGH University of Science and Technology in Krakow. Operating conditions were: accelerating voltage 20 kV, beam current 20 nA, background time 10 s and a beam diameter below 1 µm for Sn-bearing minerals and 5 µm for sphalerite. The following wavelengths were used: CdLα, InLα, ZnKα, CuKα, SKα, SnLα, HgMα, FeKα, MnKα, AgLα, GaLα, and GeLα. Natural mineral standards (FeS$_2$) and synthetic standards (CdS, InAs, ZnS, Cu, SnS, HgTe, MnS, Ag, GaP, and GeS) were used for calibration. Average detection limits are Cd 550 ppm, In 230 ppm, Zn 250 ppm, Cu 200 ppm, S 80 ppm, Sn 100 ppm, Hg 200 ppm, Fe 100 ppm, Mn 95 ppm, Ag 90 ppm, Ga 135 ppm, and Ge 140 ppm.

Trace elements analyses of sphalerite co-existing with SGM were performed at the Bulgarian Academy of Science in Sofia by laser ablation inductively-coupled plasma mass spectrometry (LA-ICP-MS). The used instrument was a 193 nm New Wave UP193FX laser ablation system coupled to an ICP-MS (Perkin-Elmer Sciex ELAN DRC-e, Waltham, MA, USA). Ablation was done using a 35 µm diameter spot size; laser energy was run at a pulse frequency of 6 Hz and pulse energy of 7.8 J·cm^{-2}. External standards NIST SRM 610 and MASS1 sulfide standard (USGS) were used for calibration. The following isotopes have been measured: Mn^{55}, Fe^{57}, Co^{59}, Ni^{62}, Cu^{65}, Zn^{66}, Ga^{69}, As^{75}, Se^{77}, Mo^{95}, Ag^{107}, Cd^{111}, In^{115}, Sn^{118}, Sb^{121}, Te^{125}, Au^{197}, Hg^{202}, Tl^{205}, Pb^{208}, and Bi^{209}. Data reduction was undertaken using Zn (determined by EPMA) as an internal standard and the SILLS v.1.1.0 software [36]. The flat shape of LA-ICP-MS spectra may suggests that the obtained Sn content in analyzed sphalerite samples correspond to its content in the crystal lattice or to the nanoinclusions not visible even in BSE images (Figure 2).

It has been shown that the equilibrium compositions of sphalerite and stannite can be used successfully as a geothermometer [15,18,37,38]. The equations given by the above authors have been applied to calculate the formation temperatures of co-existing sphalerite and SGM from various deposits.
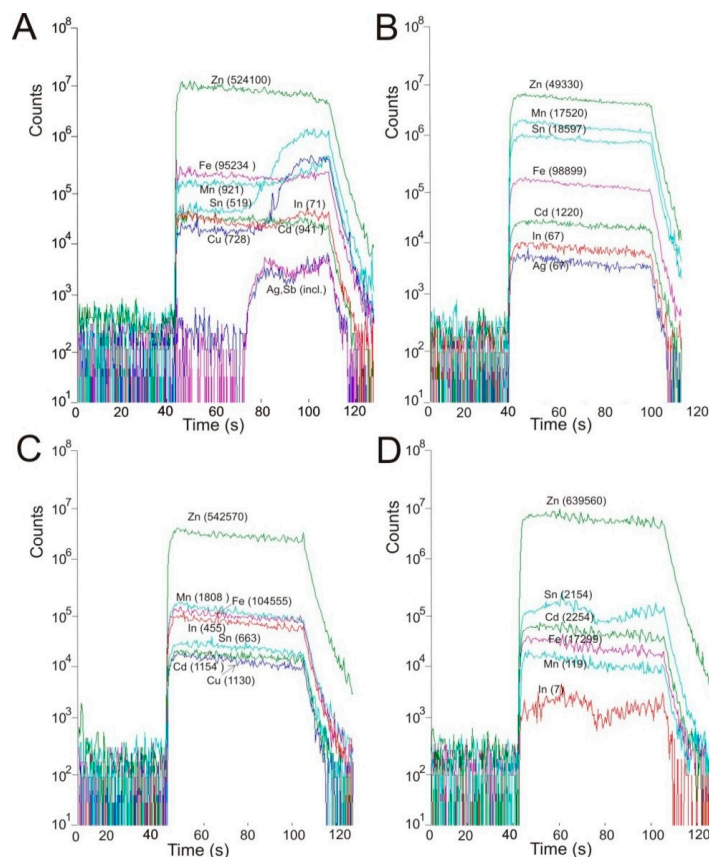
Figure 2. Examples of LA-ICP-MS time-resolved depth profiles for sphalerite from Kosovo deposits. CPS—counts per second. Numbers indicate concentration of selected elements (in ppm). (**A**) Stan Terg sphalerite with some Sn-In-Cu-Ag-Sb inclusion. Flat spectra in the first part was used to calculate concentration in sphalerite; (**B**) flat spectra of sphalerite from Artana; (**C**) flat spectra of sphalerite from Kizhnica; (**D**) spectrum of sphalerite from Drazhnje with two parts with elevated Sn and In content, possible two tiny indium-enriched SGM minerals in sphalerite.

4. Results

4.1. Mineralogy

The Pb-Zn deposits in Kosovo share a similar mineralogical signature that is typical for a metasomatic-hydrothermal origin. The main ore minerals are galena, sphalerite, pyrite, pyrrhotite, arsenopyrite, and chalcopyrite with various contents of fahlores, and associated with various sulfosalts, like boulangerite, Bi-minerals, Ag-minerals, and native elements. The gangue minerals are quartz and carbonates and, in the Stan Terg mine, also skarn minerals, like hedenbergite, wollastonite, and ilvaite are present. SGM were found in all of described deposits. Previously, stannite was identified in Stan Terg and Kizhnica by Smejkal [29,39] and there is no other evidence of other Sn-minerals in the studied deposits. Stan Terg was the best-sampled deposit, and we found SGM only in the northern part of the deposit (ore bodies 109e, 139e, and 149e).

Two stannite group minerals, namely stannite and ferrokësterite, were identified in the studied samples. Stannite in the Stan Terg deposit occurs as intergrowths with chalcopyrite in the carbonate

matrix, it is included in chalcopyrite, or fills cracks in pyrite, and is considered to be contemporaneous to chalcopyrite (Figure 3A,B). In the Artana deposit, ferrokësterite occurs in veinlets within sphalerite (Figure 3C) or along growth zones of sphalerite (Figure 3D), suggesting contemporaneous deposition of both minerals. Galena and chalcopyrite postdate sphalerite-ferrokësterite deposition (Figure 3C). Samples from Kizhnica are enriched in chalcopyrite, which postdates sphalerite-ferrokësterite (Figure 3E,F). Ferrokësterite occurs as growth zones or as single small inclusions (up to 10 μm in diameter) in sphalerite (Figure 3E,F). In the samples from the Drazhnje deposit, ferrokësterite is rimming and replaces sphalerite in boulangerite-bearing ores (Figure 3G,H).
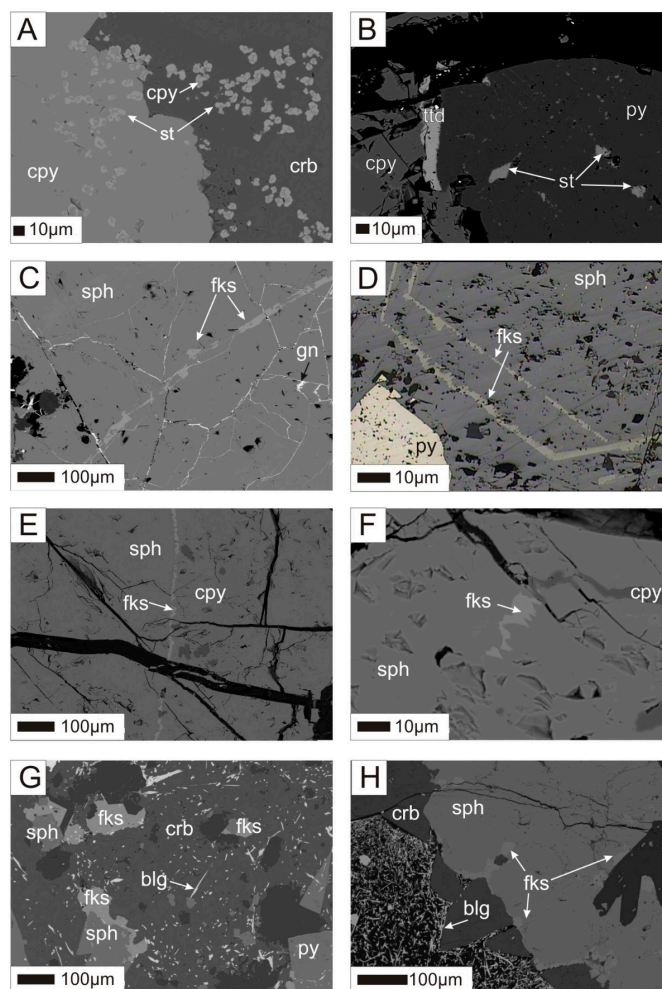
Figure 3. Microphotographs demonstrating textures of Sn-minerals in the investigated ore samples (**A**,**B**)—Stan Terg; (**C**,**D**)—Artana; (**E**,**F**)—Kizhnica; (**G**,**H**)—Drazhnje. (**A**) Fine inclusions of stannite (st) intergrown with chalcopyrite (cpy) within chalcopyrite and carbonates (crb); (**B**) stannite (st) filling up cracks in pyrite (py) grain. ttd—tetrahedrite, cpy—chalcopyrite; (**C**) ferrokësterite (fks) and galena (gn) filling cracks and veinlets in sphalerite (sph); (**D**) ferrokësterite (fks) grown zones in sphalerite (sph); (**E**) ferrokësterite (fks) exsolution marking growth zone within sphalerite (sph) accompanied by chalcopyrite inclusions (cpy); (**F**) ferrokësterite (fks) inclusion in sphalerite in association with chalcopyrite; (**G**) ferrokësterite (fks) overgrowing sphalerite grains (sph) in the carbonate matrix (crb). White needles are boulangerite (blg); (**H**) ferrokësterite (fks) overgrowing sphalerite (sph) in the zone enriched in boulangerite (blg). (**A**–**C**, **E**–**H**) — BSE images, (**D**)—reflected light crossed polaroids.
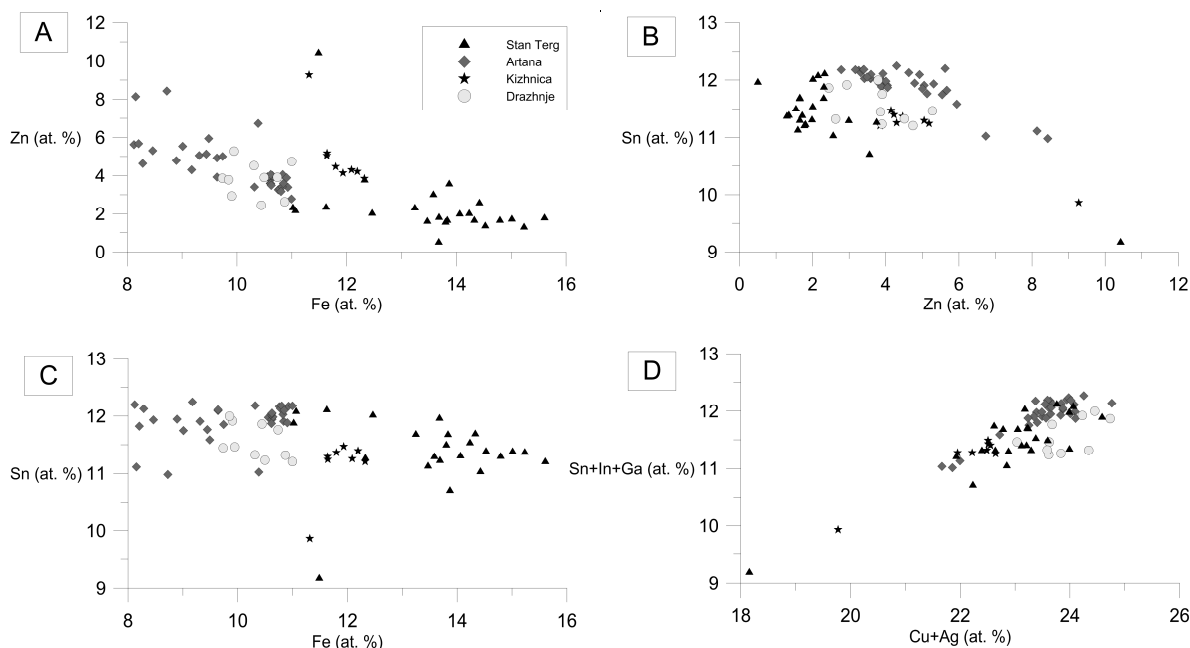
4.2. Chemical Composition of Stannite Group Minerals

Chemical composition of representative analyses of SGM from the studied deposits are presented in Table 1 and all data are plotted in Figure 4.

Table 1. Representative EPMA analyses of SGM (wt %); bd—below detection limit. Analyses 3 and 4 are examples of phase enriched in In.

Elements	Stan Terg				Artana						Kizhnica				Drazhnje			
	1	2	3	4	5	6	7	8	9	10	11	12	13	14	15	16	17	18
Cu	27.09	26.81	28.57	27.46	28.09	28.26	26.01	28.20	26.08	27.94	27.12	26.32	26.95	27.38	27.70	27.92	27.66	26.92
Fe	15.73	12.83	14.10	15.09	11.32	9.19	9.13	9.72	11.01	8.38	12.47	12.75	12.56	13.10	11.04	11.43	10.63	10.21
Zn	1.57	4.57	1.96	1.64	3.37	5.79	10.32	6.17	8.35	6.77	5.52	5.31	5.10	4.78	4.70	5.77	5.44	6.34
Sn	24.93	24.90	24.74	25.12	26.75	26.24	24.23	26.40	24.83	25.66	25.54	25.22	25.66	25.32	25.67	24.75	24.78	25.02
S	28.75	29.83	29.79	29.46	29.46	29.62	29.86	29.69	30.18	29.14	30.19	30.48	30.16	30.46	29.36	29.34	29.57	29.49
In	bd	0.06	0.43	0.65	0.27	0.09	0.07	0.04	0.01	0.10	0.08	0.05	0.05	0.03	0.02	0.04	bd	bd
Mn	0.34	0.02	bd	0.13	0.41	0.31	0.29	0.31	0.59	0.42	0.03	0.03	bd	0.02	0.17	0.19	0.28	0.25
Ag	0.29	bd	bd	bd	0.10	0.13	0.04	0.15	0.09	0.10	0.02	0.05	0.01	0.02	bd	bd	bd	0.01
Hg	bd	bd	0.03	bd	bd	bd	bd	bd	0.01	0.03	0.02	bd	bd	bd	bd	bd	bd	0.04
Ga	0.04	0.02	bd	bd	0.02	bd	bd	bd	0.01	bd	bd	bd	bd	0.05	bd	0.02	bd	bd
Total	98.74	99.04	99.62	99.55	99.79	99.63	99.95	100.68	101.16	98.54	101.76	100.21	100.49	101.16	98.66	99.46	98.36	98.28
Chemical formula based on four cations																		
Cu	1.81	1.83	1.92	1.84	1.91	1.94	1.75	1.90	1.73	1.93	1.81	1.78	1.81	1.82	1.90	1.88	1.90	1.86
Fe	1.18	0.98	1.06	1.13	0.87	0.71	0.69	0.73	0.82	0.65	0.93	0.97	0.95	0.98	0.85	0.86	0.82	0.79
Zn	0.10	0.30	0.13	0.11	0.22	0.38	0.67	0.40	0.53	0.45	0.35	0.34	0.33	0.30	0.31	0.37	0.36	0.42
Sn	0.88	0.89	0.88	0.89	0.96	0.95	0.87	0.94	0.87	0.93	0.90	0.90	0.91	0.89	0.93	0.88	0.90	0.91
S	3.74	3.96	3.91	3.83	3.92	3.96	3.92	3.90	3.91	3.93	3.93	4.03	3.96	3.96	3.93	3.85	3.97	3.97
In	0.00	0.00	0.02	0.02	0.00	0.00	0.00	0.00	0.00	0.00	0.00	0.00	0.00	0.00	0.00	0.00	0.00	0.00
Mn	0.03	0.00	0.00	0.01	0.03	0.02	0.02	0.02	0.04	0.03	0.00	0.00	0.00	0.00	0.01	0.01	0.02	0.02
Ag	0.01	0.00	0.00	0.00	0.00	0.01	0.00	0.01	0.00	0.00	0.00	0.00	0.00	0.00	0.00	0.00	0.00	0.00
Hg	0.00	0.00	0.00	0.00	0.00	0.00	0.00	0.00	0.00	0.00	0.00	0.00	0.00	0.00	0.00	0.00	0.00	0.00
Ga	0.00	0.00	0.00	0.00	0.00	0.00	0.00	0.00	0.00	0.00	0.00	0.00	0.00	0.00	0.00	0.00	0.00	0.00
X^{Fe}/X^{Zn}	11.80	3.27	8.15	10.27	3.95	1.87	1.03	1.83	1.55	1.44	2.66	2.85	2.88	3.27	2.74	2.32	2.28	1.88

Cd, Ge are below detection limits.

Figure 4. Binary plots showing chemical composition (at. %) of stannite group minerals from Kosovo Pb-Zn deposits: (**A**) Zn *vs*. Fe at. %; (**B**) Sn *vs*. Zn at. %; (**C**) Sn *vs*. Fe at. %; and (**D**) Sn + In + Ga *vs*. Cu + Ag at. %.

SGM in the Stan Terg can be classified as stannite. The Fe content varies between 11.62 and 15.23 at. %, whereas Zn between 1.30 and 3.75 at. %. Stannite contains In, Mn, and Ag in amounts up to 0.30, 0.34, and 0.14 at. %, respectively. Traces of Hg, Ga, and Ge were also detected.

SGM in the Artana deposit are classified as ferrokësterite, with Fe content ranging between 8.12 and 10.99 at. % and Zn between 2.78 and 8.42 at. %. In content is up to 0.04 at. %; Mn 0.56 at. %, Ag 0.07 at. %. and Ga and Hg reach values up to 0.03 at. %.

SGM in the Kizhnica deposit were identified as ferrokësterite, with Fe content between 11.31 and 12.32 at. %, whereas Zn was between 3.84 and 9.27 at. %. In, Mn, Ag, Hg, and Ga reach values of up to 0.04 at. %.

In Drazhnje, ferrokësterite contains Zn ranging from 2.63 to 5.27 at. % and Fe from 9.73 to 10.99 at. %. In, Hg, and Ga were measured in traces (up to 0.03 at. %).

The X^{Fe}/X^{Zn} ratio of SGM differs significantly in each of the deposits and varies from 1.10 to 27.07, 1.00 to 3.95, 1.22 to 3.21, and 1.88 to 4.27 in Stan Terg, Artana, Kizhnica, and Drazhnje, respectively. The highest content of Fe was observed in Stan Terg and the lowest in the Artana deposit (Figure 4). The incorporation of rare elements is following the Sn + In + Ga *vs.* Cu + Ag substitution scheme (Figure 4). This substitution trend is valid for all studied localities and it also applies for the coexisting sphalerite.

4.3. Chemical Composition of Sphalerite

The chemical composition of sphalerite from the studied deposits is presented in Table 2. Sphalerite is Fe-rich: the content of FeS in sphalerite from Stan Terg ranges between 15 and 25 moles %, from Artana, between eight and 20 moles %, and from Kizhnica, between 16 and 21 moles %. Sphalerite from Drazhnje has a significant lower content of FeS in the range from 2.6 to 6 moles %.

Table 2 demonstrates a large variation in trace element content of sphalerite coexisting with SGM measured by LA-ICP-MS. The results are plotted in Figures 5 and 6.

Table 2. Representative LA-ICP-MS analyses of sphalerite coexisting with SGM (ppm) and mean EPMA analyses (wt %). Zn is from EPMA.

Elements	Stan Terg		EPMA	Artana		EPMA	Kizhnica		EPMA	Drazhnje		EPMA
Zn	524,100	547,800	53.42	543,380	563,160	55.80	544,690	542,570	53.94	645,600	654,430	63.97
Fe	95,234	92,029	11.37	76,359	100,781	11.31	115,454	104,555	11.88	23,947	17,635	2.59
Mn	699	1,196	0.16	22,879	19,515	1.97	1,337	1,808	0.18	260	126	0.21
Cd	921	892	0.06	1,331	1,351	0.06	1,313	1,154	0.04	1,428	1,575	0.14
Sn	519	6.8	0.21	5,936	286	1.66	316	663	0.03	2,787	267	0.05
Cu	728	101	0.85	6,288	474	1.86	973	1,130	0.08	2,215	398	0.14
In	71	36	0.03	40	11	bd	730	455	0.05	8.4	0.88	bd
Co	3.4	1.2	n.a.	<0.29	<0.20	n.a.	2.1	2.3	n.a.	32.3	37	n.a.
Hg	3.8	11	bd	26	22	bd	13	13	bd	62	6	0.02
Ga	2.4	1.1	bd	101	76	bd	0.78	1.4	bd	4.8	2.5	bd
Ag	2.0	0.88	bd	23	2.1	bd	2.5	2.9	bd	0.97	1.2	bd
S	n.a.	n.a.	32.91	n.a.	n.a.	33.34	n.a.	n.a.	33.84	n.a.	n.a.	32.44

Se, Mo, Te, Ta, Tl, W, Pb, Au, Bi, As, and Sb are below minimum detection limit. n.a.—not analyzed; bd—below detection limit.
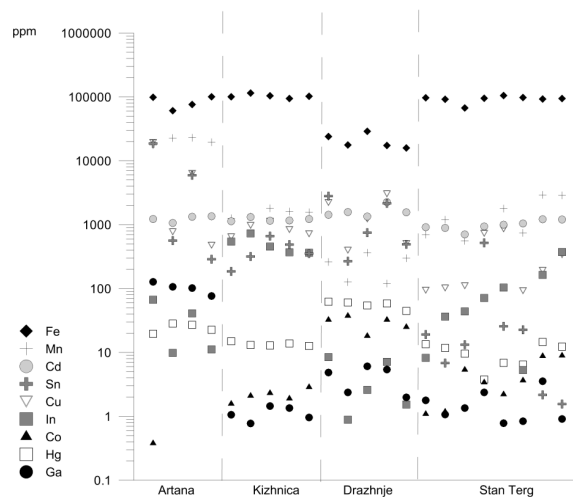
Figure 5. Comparison of sphalerite composition from Artana, Kizhnica, Drazhnje, and Stan Terg. Values obtained by LA-ICP-MS (in ppm).
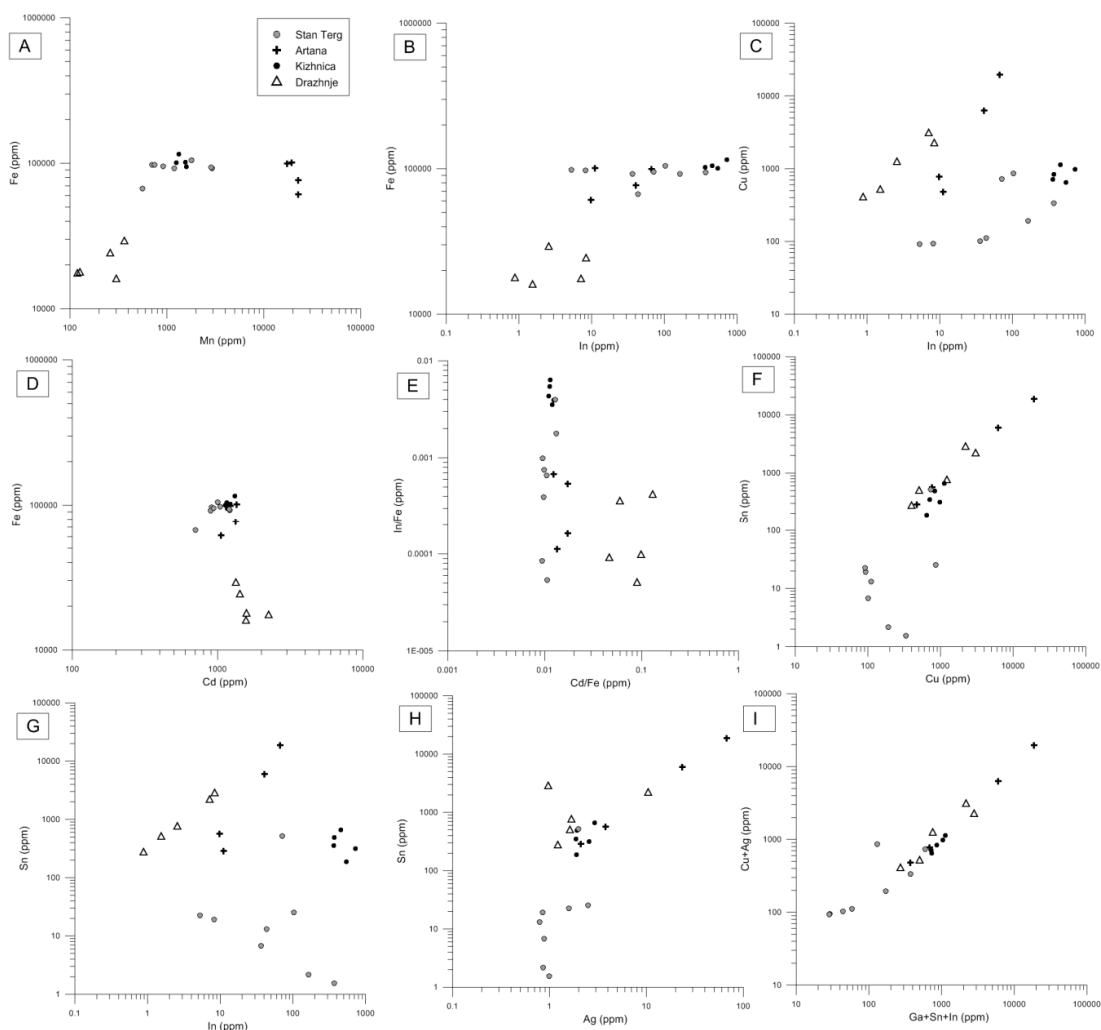
Figure 6. Binary plots showing chemical composition (ppm) of sphalerite from Kosovo Pb-Zn deposits: (**A**) Fe *vs.* Mn; (**B**) Fe *vs.* In; (**C**) Cu *vs.* In; (**D**) Fe *vs.* Cd; (**E**) In/Fe *vs.* Cd/Fe; (**F**) Sn *vs.* Cu; (**G**) Sn *vs.* In; (**H**) Sn *vs.* Ag; and (**I**) Cu + Ag *vs.* Ga + Sn + In.

Tin content in the sphalerite coexisting with stannite in the Stan Terg deposit is only a few ppm, which is the lowest measured value. Occasionally, and proximal to SGM, the content of Sn could be high (up to 520 ppm). The content of Sn in the other localities is significantly higher. The maximum value (up to 2800 ppm) was measured in the Drazhnje deposit. The content in Artana and Kizhnica is intermediate—1600 and 663 ppm, respectively.

Manganese was mostly enriched in sphalerite from Artana, that is 2.06 wt % in average. In Kizhnica and Stan Terg these values are lower, 1511 and 1463 ppm, respectively. Manganese content in Drazhnje is very minor—average 233 ppm. Content of Co is negligible and it was recorded in Kizhnica, Stan Terg, and Drazhnje with 2.14, 4.3, and 29 ppm in average. The most noticeable Ga content (102 ppm) is present in sphalerite from Artana, and the highest In content (492 ppm) was measured in sphalerite from Kizhnica. Slightly elevated Ag content was found in Artana (up to 64 ppm). Cadmium is abundant with relatively elevated contents (in average 0.12 wt % in Artana and in Kizhnica, 0.16 wt % in Drazhnje, and 0.10 wt % in Stan Terg).

5. Discussion

5.1. Stannite-Kësterite Solid Solution

Stannite is the most common tin sulfide mineral. Stannite-kësterite solid solution was studied by numerous authors and commonly occurs in numerous polymetallic deposits of various genetic types, e.g., by Kissin and Owens [40], Kissin [41], and Bonazzi *et al.* [42]. Stannite is the iron-rich member with the chemical formula Cu_2FeSnS_4, whereas kësterite is the zinc-dominant end member with an empirical formula $Cu_2(Zn,Fe)SnS_4$. The intermediate member with a prevalence of Fe over Zn is known as ferrokësterite $Cu_2(Fe,Zn)SnS_4$.

The crystal structure of stannite and kësterite was determined by Hall *et al.* [43]. They investigated the structural differences due to the positioning of the Cu atoms at the distinct unit cells and the optical properties of these two minerals. Kissin and Owens [40] and Kissin [41] supposed the presence of a miscibility gap in stannite-kësterite solid solution. Bonazzi *et al.* [42] studied the mechanism of incorporation of Cu, Fe, and Zn in the stannite-kësterite series, based on analyses of synthesized crystals. They supported the hypothesis that stannite and kësterite crystallize in two different space groups with (Fe, Zn) and Cu on different positions. They noticed the discontinuity in the cell-parameter plot. Isomorphic substitution mechanism and full solid solution between stannite and kësterite was confirmed by the mean of Mössbauer spectroscopy [44,45].

Numerous chemical compositions of stannite and kësterite were documented by Springer [46] from Bolivia, Cornwall, and Zinnwald. Springer indicated that iron can be commonly substituted by zinc, as well as the atomic ratio Cu:(Fe + Zn):Sn is not always 2:1:1, but the metal:sulfur ratio remains always 1:1. He noticed that if ZnS is included in stannite, the Cu and Sn are simultaneously decreasing. Similar results confirming chemical composition of phases between stannite and kësterite were documented by Moore and Howie [47] from Cornwall. They identified kësterite, zincian stannite, and the Cu-enriched phase stannoidite. Nekrasov *et al.* [15] indicated that Zn enrichment in stannite may reach the point of kësterite formation according to the equation: $Cu_2FeSnS_4 + ZnS \rightarrow Cu_2ZnSnS_4 + FeS$.

Recently numerous modern analytical techniques were applied to investigate stannite-kësterite solid solution. Evstigneeva *et al.* [48] studied isomorphic substitution mechanism in the SGM by the mean of a microprobe and profile analysis (Rietveld method), Mossbauer spectroscopy, scanning, and transmitting electron microscopy, and X-ray photoelectron spectroscopy, and Schorr *et al.* [49] simultaneously applied Rietveld analysis of X-ray and neutron powder diffraction data. According to [48] the Fe-Cu replacement on synthetic samples requires Fe^{3+} in order to achieve charge balance, however, in natural samples most of the charge balance is achieved by divalent Fe ions.

The composition of the investigated Sn-minerals from Kosovo is shown in Figure 7. Most of the measured phases fall within the ferrokësterite field. Phases measured in the Stan Terg samples

have the closest formulae to the ideal stannite. In most of the analyzed SGM it appears to be about 0.15–0.20 atoms per formula unit (*apfu*) Cu deficiency. Similar depletion was noticed by Catchpole *et al.* [8] in samples from Peru. Stannite from Stan Terg with increased In content (up to 0.02 *apfu*) could alternatively be petrukite, a phase with similar chemical composition to stannite, e.g., $(Cu,Fe,Zn)_3(Sn,In)S_4$, but with different symmetry. Petrukite is a rare Sn-bearing mineral occurring in only a few localities world-wide [11,22,40]. Radosavljevic *et al.* [22] described a petrukite occurrence in the Srebrenica locality, located within the Vardar Zone, but north from the Trepça Mineral Belt. The average chemical formula given for Srebrenica is $(Cu_{1.96},Fe_{0.98},Zn_{0.09},Ag_{0.01})_{\Sigma3.04}(Sn_{0.94}, In_{0.02})_{\Sigma0.96}S_{3.99}$. The phase No. 3 in Table 1 from Stan Terg has a formula $(Cu_{1.92},Fe_{1.06},Zn_{0.13})_{\Sigma3.11}(Sn_{0.88}, In_{0.02})_{\Sigma0.90}S_{3.91}$, which is in good agreement with the phase described from Srebrenica. However, the presence of petrukite in the Stan Terg cannot be confirmed without X-ray structural analyses.
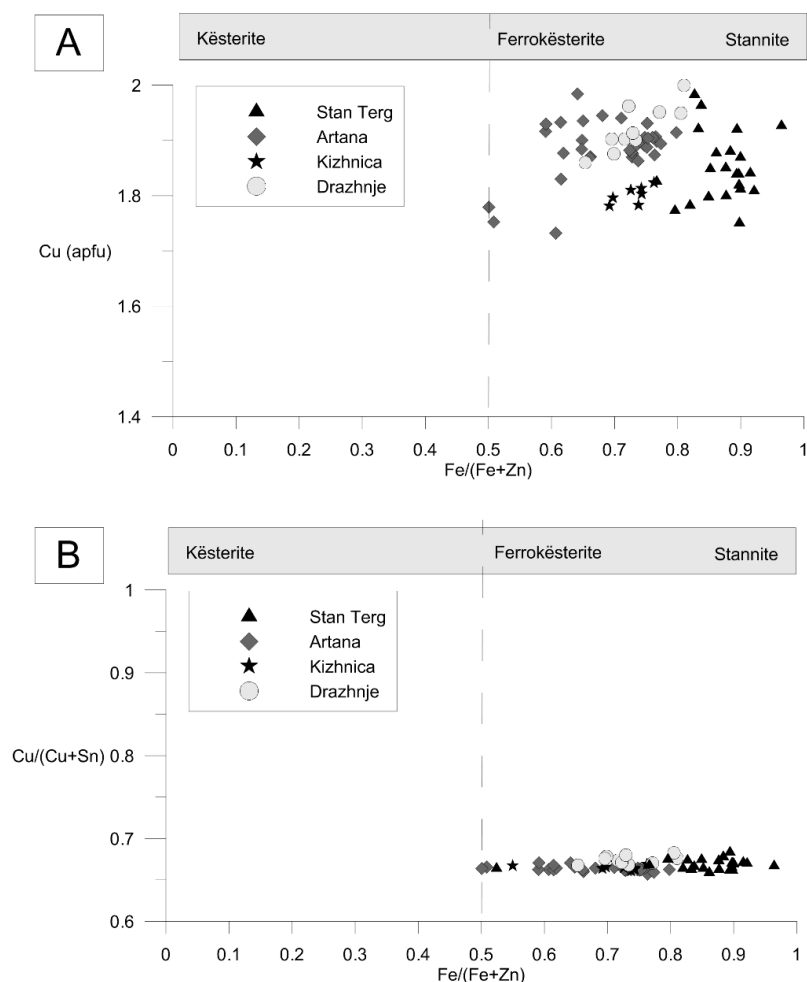

Figure 7. Chemical composition of stannite group minerals from Kosovo deposits as a function of (**A**) Cu *vs*. Fe/(Fe + Zn); and (**B**) Cu/(Cu + Zn) *vs*. Fe/(Fe + Zn). Grey boxes indicate the approximate fields of stability for stannite-kësterite solid solution regarding Fe/(Fe + Zn).

5.2. Implication for Ore Precipitation Conditions

Coexisting stannite and sphalerite have been considered by numerous authors as a good geothermometer, and are used in this work to estimate precipitation conditions of described phases.

Using the equation of Nakamura and Shima [17] on the partitioning of Fe and Zn between coexisting sphalerite and stannite group minerals (Figure 8), we obtained the following ore-forming temperatures for the studied deposits: 240–390 °C (Stan Terg), 320–370 °C (Artana), >340 °C (Kizhnica),

and 245–295 °C (Drazhnje). The estimated temperatures are comparable to those reported above for coexisting pairs of stannite group minerals and sphalerite. Drazhnje reveals lower temperatures than those obtained from the other deposits, probably due to a different composition of sphalerite (e.g., lower Fe content, Hg- and Co-enrichment, *etc*.) compared to the other occurrences. The distinct chemistry of Drazhnje sphalerite may be related not only to local, but also to regional processes, reflecting distinct origin (e.g., different metallogenic areas for the deposits): Artana, Stan Terg, and Kizhnica are lying in the central metallogenic belt connected with the Vardar zone, whereas Drazhnje is connected with the external, eastern metallogenic zone and with the Lece volcanic complex.
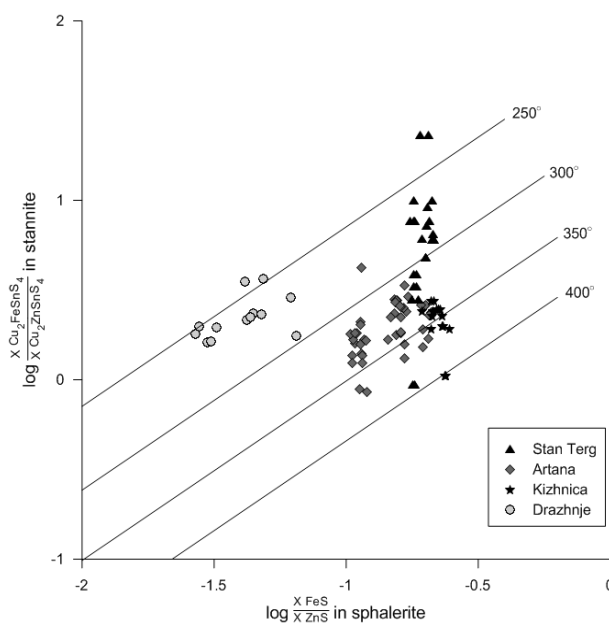
Figure 8. Log (XFeS/XZnS)sphalerite–log (XCu$_2$FeSnS$_4$/XCu$_2$ZnSnS$_4$) stannite diagram showing results for sphalerite and stannite from Kosovo deposits. Temperature lines are based on data by Nakamura and Shima [17].

It is suggested here that sphalerite and stannite group minerals in Kosovo precipitated simultaneously during cooling of the hydrothermal fluids, as indicated by the wide range of the obtained temperatures. However, the precipitation of Sn-bearing minerals occurring in growth zones in sphalerite could mark fluctuations in physico-chemical conditions of the ore fluids, e.g., temperature variations, inflow of Sn-bearing solutions, *etc*. and may correlate to short intervals of magmatic pulses in the mineralization. This is best demonstrated for the Artana deposit, where SGM occur in veinlets within sphalerite, or clearly marking grow zones of sphalerite, suggesting changes in precipitation conditions. In accordance to that stated by Kołodziejczyk *et al*. [25] for Stan Terg deposit, sphalerite and stannite group minerals in all studied mineralization were deposited under reduced conditions under low-sulfidation fluid states.

5.3. Partitioning of Sn, Zn, and Fe into Sphalerite and Sn-Bearing Sulfide

Numerous trace element studies in sphalerite indicated that Sn commonly occurs as a minor element [50–52]. However, Evrard *et al*. [53] documented up to 6 wt. % Sn in sphalerite from the Logatchev submarine hydrothermal field (and assigned it to stannite inclusions), Mid-Atlantic Range, and Ono *et al*. [54] measured 1.8–4.3 wt % Sn in sphalerite from polymetallic mineralization at the Suttsu vein-type deposit in Japan. Sphalerite analyzed by LA-ICP-MS at various base metal bearing deposits from South China [52], revealed very low Sn content (up to 10 ppm), only in one deposit (e.g., the Bainiuchang VMS deposit) the Sn content in average 1130 ppm, but this could be due to the small size of the Sn-bearing minerals. Cook *et al*. [51] summarized the LA-ICP-MS trace element data

of sphalerite and indicated that Sn content is very low in samples from skarn and stratabound deposits, but it might increase in sphalerite from epithermal systems, where it reaches values of up to 1.17 wt % at Toyoha Cu-Zn-In deposit, in Japan. The flat spectra obtained in these studies rather suggest an incorporation of Sn into the sphalerite lattice and are not attributed to mineral inclusions in sphalerite.

Various ways of incorporation of Sn, Cu, and In into sphalerite can be considered following the binary chemical plots in Figure 6. The positive correlation between Cu and Sn in all localities, with the exception of the Stan Terg deposit (Figure 6H), suggests incorporation of Sn in a tetravalent state through $2(Cu^+Ag^+) + Sn^{4+} \leftrightarrow 3Zn^{2+}$ substitution, in accordance to the statement of [51]. Alternatively, the correlation between Sn and Cu could be also attributed to sub-microscopic stannite- or kuramite-like domains in the sphalerite structure. Indium content correlates with Cu in all samples suggesting the coupled $(Cu^+In^{3+}) \leftrightarrow 2Zn^{2+}$ substitution or, alternatively, the occurrence of roquesite-like domains in sphalerite (Figure 6C). In the sphalerites from Stan Terg there is a negative trend between Sn and In (Figure 6G), possibly indicating In for Sn substitution in petrukite micro-inclusions of sphalerite.

Dobrovol'skaya *et al.* [55] described from different Sn deposits rare myrmekitic stannite-sphalerite intergrowths caused by ore metamorphism at the contact with a dyke. Stannite measured by them contained 3.61–5.75 wt % Zn, whereas the Sn content in co-existing sphalerite is up to 0.46 wt %. In Kosovo, sample Sn minerals commonly occur within sphalerite in the form of blebs, as continuous stannite growth zones, or overgrowing and replacing sphalerite.

Oen *et al.* [56] noticed discontinuous solid solutions in the $(Zn,Fe)S–Cu_2FeSnS_4–CuInS_2$ system. They described oscillatory zoning in sphalerite containing stannite inclusions in ore samples from J. Cesar deposit (Spain) and explained them by possible fluctuations in fluid temperatures. Similar grown zones composed of stannite have been found in samples from the Artana deposit (this study). The change from stannite to sphalerite precipitation occurred at the point when the hydrothermal fluids become sufficiently rich in ZnS to precipitate sphalerite.

6. Concluding Remarks

1. Tin mineralization is very similar in the Trepça Mineral Belt among different deposits. Only members of stannite-kësterite solid solution were found, and there is no evidence of presence other Sn-minerals enriched in Cu, Ag, Cd, In, or Ge. In a few samples from Stan Terg a phase enriched in In (0.02 *apfu*) was found and it could fit petrukite.

2. The chemical composition of stannite group minerals indicates extensive mutual substitution between Fe and Zn. In the coexisting sphalerites correlations between Sn, Cu, and In, suggest either incorporation of these elements in the structrure, and/or the presence of stannite, kuramite, roquesite, and petrukite micro-inclusions in sphalerite.

3. Estimated temperatures on the basis of coexisting sphalerite-stannite group minerals, indicate a wide range of ore precipitation in each deposit: 240–390 °C (Stan Terg), 240–370 °C (Artana), >340 °C (Kizhnica), and 245–295 °C (Drazhnje). Although sphalerite and Sn-minerals precipitated simultaneously during cooling of the hydrothermal fluids, oscillatory zoning in sphalerite (as evidenced by ferrokësterite growth zones) suggests fluctuation in physico-chemical conditions, and short-time intervals of magmatic pulses.

4. Tin-bearing minerals and sphalerite at Kosovo contain small amounts of In, Ga, and Ge, and may be considered as potential carriers of critical metals in the district with implication for future exploration.

Author Contributions: Joanna Kołodziejczyk, Jaroslav Pršek and Burim Asllani collected the research material; Joanna Kołodziejczyk and Jaroslav Pršek performed EPMA study; Joanna Kołodziejczyk collected LA-ICP-MS data; Joanna Kołodziejczyk, Jaroslav Pršek, Panagiotis Voudouris and Vasilios Melfos analyzed the data and wrote the paper.

Conflicts of Interest: The authors declare no conflict of interest.

Abbreviations

The following abbreviations are used in this manuscript:

SGM	Stannite Group Minerals
TMB	Trepça Mineral Belt
LA-ICP-MS	Laser ablation inductively coupled plasma mass spectrometry

References

1. Kesler, S.E.; Wilkinson, B.H. Tectonic-diffusion estimates of global minerals resources: Extending the method: Granitic tin deposits. In *Ore Deposits in an Evolving Earth*; Jenkin, G.R.T., Lusty, P.A.J., McDonald, I., Smith, M.P., Boyce, A.J., Wilkinson, J.J., Eds.; Geological Society: London, UK, 2013; Volume 393, pp. 277–290.

2. Ishibashi, M. A Sn-Te-Bi-Sb paragenesis in ores from the suttsu mine, Hokkaidô. *J. Fac. Sci. Hokkaido Univ.* **1952**, *8*, 97–106.

3. Wenyuan, L.; Cook, N.J.; Ciobanu, C.L.; Yu, L.; Xiaoping, Q.; Yuchuan, C. Mineralogy of tin-sulfides in the Zijinshan porphyry–epithermal system, Fujian Province, China. *Ore Geol. Rev.* **2016**, *72*, 682–698. [CrossRef]

4. Novák, F.; Blüml, A.; Tacl, A. The origin of stannite by replacement of cassiterite in the Turkaňk zone of the Kutná Hora ore deposit. *Mineral. Mag.* **1962**, *33*, 339–342. [CrossRef]

5. Kettaneh, Y.A.; Badham, J.P.N. Mineralization and paragenesis at the Mount Wellington Mine, Cornwall. *Econ. Geol.* **1978**, *73*, 486–495. [CrossRef]

6. Benzaazoua, M.; Marion, P.; Pinto, A.; Migeon, H.; Wagner, F.E. Tin and indium mineralogy within selected samples from the Neves Corvo ore deposit (Portugal): A multidisciplinary study. *Miner. Eng.* **2003**, *16*, 1291–1302. [CrossRef]

7. Brill, B.A. Trace-element contents and partitioning of elements in ore minerals from the CSA Cu–Pb–Zn deposit, Australia. *Can. Mineral.* **1989**, *27*, 263–274.

8. Catchpole, H.; Kouzmanov, K.; Fontboté, L. Copper-excess stannoidite and tennantite-tetrahedrite as proxies for hydrothermal fluid evolution in a zoned Cordilleran base metal district, Morococha, central Peru. *Can. Mineral.* **2012**, *50*, 719–743. [CrossRef]

9. Kase, K. Tin, Arsenic, Zinc and Silver vein mineralization in the Besshi mine, central Shikoku. *Min. Geol.* **1988**, *38*, 407–418.

10. Petruk, W. Tin sulphides from the deposit of Brunswick Tin Mines Limited. *Can. Mineral.* **1973**, *12*, 46–54.

11. Voudouris, P.; Melfos, V.; Spry, P.G.; Bonsall, T.A.; Tarkian, M.; Solomos, Ch. Carbonate-replacement Pb–Zn–Ag $\pm$ Au mineralization in the Kamariza area, Lavrion, Greece: Mineralogy and thermochemical conditions of formation. *Mineral. Petrol.* **2008**, *94*, 85–106. [CrossRef]

12. Voudouris, P.; Melfos, V.; Spry, P.G.; Moritz, R.; Papavassiliou, K.; Falalakis, G. Mineralogy and geochemical environment of formation of the Perama Hill high-sulfidation epithermal Au-Ag-Te-Se deposit, Petrota Graben, NE Greece. *Mineral. Petrol.* **2011**, *103*, 79–100. [CrossRef]

13. Repstock, A.; Voudouris, P.; Kolitsch, U. New occurrences of watanabeite, colusite, "arsenosulvanite" and Cu-excess tetrahedrite-tennantite at the Pefka high-sulfidation epithermal deposit, northeastern Greece. *Neues Jahrb. Mineral. Abh.* **2015**, *192*, 135–149. [CrossRef]

14. Zarić, P.; Janković, S.; Radosavljević, S.; Dordević, D. Tin minerals and tin mineralization of the Pb-Zn-Sb-Ag ore deposits of the Srebrenica orefield. In *Proceedings of the International Symposium Geology and Metallogeny of the Dinarides and the Vardar Zone*; Academy of Sciences and Arts of the Republic of Srpska: Banja Luka, Bosnia and Herzegovina, 2000; pp. 425–434.

15. Nekrasov, I.Y.; Sorokin, V.I.; Osadchii, E.G. Fe and Zn partitioning between stannite and sphalerite and its application in geothermometry. *Phys. Chem. Earth* **1979**, *11*, 739–742. [CrossRef]

16. Springer, G. The pseudobinary system Cu_2FeSnS-Cu_2ZnSnS_4 and its mineralogical significance. *Can. Mineral.* **1972**, *11*, 535–541.

17. Nakamura, Y.; Shima, H. Fe and Zn partitioning between sphalerite and stannite. In *Proceedings of the Joint Meeting of Society of Mining Geologists of Japan*; The Japanese Association of Mineralogists, Petrologists and Economic Geologists and the Mineralogical Society of Japan: Sendai, Japan, 1982. (In Japanese)

18. Shimizu, M.; Shikazono, N. Iron and zinc partitioning between coexisting stannite and sphalerite: A possible indicator of temperature and sulfur fugacity. *Miner. Depos.* **1985**, *20*, 314–320. [CrossRef]

19. Wagner, T.; Mlynarczyk, M.S.; Williams-Jones, A.E.; Boyce, A.J. Stable isotope constraints on ore formation at the San Rafael tin-copper deposit, Southeast Peru. *Econ. Geol.* **2009**, *104*, 223–248. [CrossRef]

20. Watanabe, M.; Hoshino, K.; Myint, K.K.; Miyazaki, K.; Nishido, H. Stannite from the Otoge kaolin-pyrophyllite deposits, Yamagata Prefecture, NE Japan and its genetical significance. *Resour. Geol.* **1994**, *44*, 439–444.

21. Ohta, E. Occurrence and chemistry of indium-containing minerals from the Toyoha mine, Hokkaido, Japan. *Min. Geol.* **1989**, *39*, 355–372.

22. Radosavljevic, S.A.; Rakic, S.M.; Stojanovic, J.N.; Radosavljevic-Mihajlovic, A.S. Occurrence of Petrukite in Srebrenica Orefield, Bosnia and Herzegovina. *Neues Jahrb. Mineral. Abh.* **2005**, *181*, 21–26. [CrossRef]

23. Féraud, J.; Deschamps, Y. *French Scientific Cooperation 2007–2008 on the Trepça Lead-Zinc-Silver Mine and the Gold Potential of Novo Brdo/Artana Tailings (Kosovo)*; BRGM Report No RP-57204-FR; BRGM: Orléans, France, 2009; p. 92.

24. Strmić Palinkaš, S.; Palinkaš, L.A.; Renac, C.; Spangenberg, J.E.; Lüders, V.; Molnar, F.; Maliqi, G. Metallogenic model of the Trepča Pb-Zn-Ag Skarn deposit, Kosovo: Evidence from fluid inclusions, rare earth elements, and stable isotope data. *Econ. Geol.* **2013**, *108*, 135–162. [CrossRef]

25. Kołodziejczyk, J.; Pršek, J.; Melfos, V.; Voudouris, P.C.; Maliqi, F.; Kozub-Budzyń, G. Bismuth minerals from the Stan Terg deposit (Trepça, Kosovo). *Neues Jahrb. Mineral. Abh.* **2015**, *192*, 317–333.

26. Lehmann, S.; Barcikowski, J.; Von Quadt, A.; Gallhofer, D.; Peytcheva, I.; Heinrich, C.A.; Serafimovski, T. Geochronology, geochemistry and isotope tracing of the Oligocene magmatism of the Buchim–Damjan–Borov Dol ore district: Implications for timing, duration and source of the magmatism. *Lithos* **2013**, *180–181*, 216–233. [CrossRef]

27. Hyseni, M.; Durmishaj, B.; Fetahaj, B.; Shala, F.; Berisha, A.; Large, D. Trepça Ore Belt and Stan Terg mine—Geological overview and interpretation, Kosovo (SE Europe). *Geologija* **2010**, *51*, 87–92. [CrossRef]

28. Forgan, C.B. Ore deposits at the Stan Terg lead-zinc mine International Geological Congress. In *The Geology, Paragenesis, and Reserves of Ores of Lead and Zinc*; Co-operative Wholesale Society Ltd.: Reddish, UK, 1948; Volume 7, pp. 290–307.

29. Smejkal, S. Structure, Mineralization, Mineralogical Parageneses and Genesis of Lead-Zinc Deposits of Kopaonic District. Ph.D. Thesis, Faculty of Mining and Geology University of Belgrade, Beograd, Serbia, 1960. (In Serbo-Croatian)

30. Jankovic, S. The isotopic composition of lead in some Tertiary lead-zinc deposits within the Serbo-macedonian metallogenic province (Yugoslavia). *Ann. Geol. Pénins. Balk.* **1978**, *42*, 507–525.

31. Jankovic, S. The principal metallogenic features of the Kopaonik District. In Proceedings of the Geology and Metallogeny of the Kopaonik Mt Symposium, Belgrade, Serbia, 19–22 June 1995; pp. 79–101.

32. Simić, M. Metallogeny of the Dražnja-Propaštica-Novo Brdo ore field in the Vardar Zone. In *Proceedings of the International Symposium Geology and Metalogeny of the Dinarides and the Vardar Zone*; Academy of Sciences and Arts of the Republic of Srpska: Banja Luka, Bosnia and Herzegovina, 2000; Volume 1, pp. 409–424.

33. Dangić, A. Minor element distribution between galena and sphalerite as a geothermometer—Application to two lead-zinc areas in Yugoslavia. *Econ. Geol.* **1985**, *80*, 180–183. [CrossRef]

34. Durmishaj, B.; Tashko, A.; Sinojmeri, A.; Neziraj, A. Chemical composition of mineral phases form Hajvalja, Badovc and Kizhnica (Kosovo). *Bul. Shk. Gjeol.* **2006**, *2*, 91–100. (In Albanian)

35. Popović, R. Distribution of base and precious metals in the Lece volcano-intrusive massif (Vardar Zone). In *Proceedings of the International Symposium Geology and Metalogeny of the Dinarides and the Vardar Zone*; Academy of Sciences and Arts of the Republic of Srpska: Banja Luka, Bosnia and Herzegovina, 2000; Volume 1, pp. 443–452.

36. Guillong, M.; Meier, D.L.; Allan, M.M.; Heinrich, C.A.; Yardley, B.W.D. Appendix A6: SILLS: A MATLAB-based program for the reduction of laser ablation ICP-MS data of homogeneous materials and inclusions. In *Laser Ablation ICP-MS in the Earth Sciences: Current Practices and Outstanding Issues*; Sylvester, P., Ed.; Mineralogical Association of Canada Short Course 40; Mineralogical Association of Canada: Vancouver, BC, Canada, 2008; pp. 328–333.

37. Nekrasov, I.Y.; Sorokin, V.I.; Osadchii, E.G. Partition of iron and zinc between sphalerite and stannite at T = 300 to 500 °C and P = 1 kb. *Dokl. Earth Sci.* **1976**, *226*, 136–138.

38. Bortnikov, N.S.; Zaozerina, O.N.; Genkin, A.D.; Muravitskaya, G.N. Stannite-sphalerite intergrowths—Possible indicators of conditions of ore deposition. *Int. Geol. Rev.* **1990**, *32*, 1132–1144. [CrossRef]

39. Smejkal, S. Lead-zinc deposits of the Tetriary metallogeny in the Kopaonik area. In *Excursion Guide. Savez Geoloških Društava FNRJ*; Savjetovanje Geologa FNRJ: Beograd, Serbia, 1962; pp. 51–58.

40. Kissin, S.A.; Owens, D.R. New data on stannite and related tin sulfide minerals. *Can. Mineral.* **1979**, *17*, 125–135.

41. Kissin, S.A. A reinvestigation of the stannite (Cu_2FeSnS_4)–kësterite (Cu_2ZnSnS_4) pseubinary system. *Can. Mineral.* **1989**, *27*, 689–697.

42. Bonazzi, P.; Bindi, L.; Bernardini, G.; Menchetti, S. A model for the mechanism of incorporation of Cu, Fe and Zn in the stannite–kësterite series, Cu_2FeSnS_4–Cu_2ZnSnS_4. *Can. Mineral.* **2003**, *41*, 639–647. [CrossRef]

43. Hall, S.R.; Szymanski, J.T.; Stewart, J.M. Kësterite, $Cu_2(Zn,Fe)SnS_4$ and stannite, Cu_2 (Fe,Zn) SnS_4, structurally similar but distinct minerals. *Can. Mineral.* **1978**, *16*, 131–137.

44. Di Benedetto, F.; Bernardini, G.P.; Borrini, D.; Lottermoser, W.; Tippelt, G.; Amthauer, G. ^{57}Fe- and ^{119}Sn-Mössbauer study on stannite (Cu_2FeSnS_4)–kesterite (Cu_2ZnSnS_4) solid solution. *Phys. Chem. Miner.* **2005**, *31*, 683–690. [CrossRef]

45. Rusakov, V.S.; Chistyakova, N.I.; Burkovsky, I.A.; Gapochka, A.M.; Evstigneeva, T.L.; Schorr, S. Mössbauer study of isomorphous substitutions in $Cu_2Fe_{1-x}Cu_xSnS_4$ and $Cu_2Fe_{1-x}Zn_xSnS_4$ series. *J. Phys.* **2010**, *217*. [CrossRef]

46. Springer, G. Electronprobe analyses of stannite and related tin minerals. *Miner. Mag.* **1968**, *36*, 1045–1051. [CrossRef]

47. Moore, F.; Howie, R.A. Tin-bearing sulphides from St Michael's Mount and Cligga Head, Cornwall. *Miner. Mag.* **1984**, *48*, 389–396. [CrossRef]

48. Evstigneeva, T.L.; Rusakov, V.S.; Kabalov, Y.K. Isomorphism in the minerals of the stannite family. *New Data Miner.* **2003**, *38*, 65–70.

49. Schorr, S.; Hoebler, H.J.; Tovar, M. A neutron diffraction study of the stannite-kesterite solid solution series. *Eur. J. Mineral.* **2007**, *19*, 65–73. [CrossRef]

50. Stoiber, R.E. Minor elements in sphalerite. *Econ. Geol.* **1940**, *35*, 501–519. [CrossRef]

51. Cook, N.J.; Ciobanu, C.L.; Pring, A.; Skinner, W.; Shimizu, M.; Danyushevsky, L.; Saini-Eidukat, B.; Melcher, F. Trace and minor elements in sphalerite: A LA-ICPMS study. *Geochim. Cosmochim. Acta* **2009**, *73*, 4761–4791. [CrossRef]

52. Ye, L.; Cook, N.J.; Ciobanu, C.L.; Liu, Y.P.; Zhang, Q.; Gao, W.; Yang, Y.L.; Danyushevsky, L.V. Trace and minor elements in sphalerite from base metal deposits in South China: A LA-ICPMS study. *Ore Geol. Rev.* **2011**, *39*, 188–217. [CrossRef]

53. Evrard, C.; Fouquet, Y.; Moëlo, Y.; Rinnert, E.; Etoubleau, J.; Langlade, J.A. Tin concentration in hydrothermal sulphides related to ultramafic rocks along the Mid-Atlantic Ridge: A mineralogical study. *Eur. J. Mineral.* **2015**, *27*, 627–638. [CrossRef]

54. Ono, S.; Hirai, K.; Matsueda, H.; Kabashima, T. Polymetallic mineralization at the Suttsu vein-type deposit, southwestern Hokkaido, Japan. *Resour. Geol.* **2004**, *54*, 453–464. [CrossRef]

55. Dobrovol'skaya, M.G.; Genkin, A.D.; Bortnikov, N.S.; Golovanova, T.I. Unusual sphalerite, chalcopyrite, and stannite intergrowths at tin deposits. *Geol. Ore Depos.* **2008**, *50*, 75–85. [CrossRef]

56. Oen, I.S.; Kager, P.; Kieft, C. Oscillatory zoning of a discontinuous solid-solution series: Sphalerite-stannite. *Am. Mineral.* **1980**, *65*, 1220–1232.